Thus the bond length should increase.

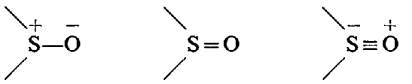

(I) (II) (III)

This is found to be the case, though the effect is quite small. Thus, the S–O bond length uncorrected for thermal motion reported by Thomas, Shoemaker & Eriks is 1·513 (5) Å, while in *trans*-$[FeCl_2(DMSO)_4]^+$ we find 1·541 (6). In BF_3(DMSO) McGandy reported a distance of 1·52 (1) Å, which differs insignificantly from that in DMSO itself and thus left unresolved the question of whether there is any increase in length upon coordination *via* oxygen. Our results show that there is indeed a small effect of this nature.

We gratefully acknowledge financial support of this work by the U.S. Atomic Energy Commission under Contract AT(30-1)-1965 and the National Science Foundation under Grants 3727 and 4329. Generous allotments of computer time by the Massachusetts Institute of Technology were indispensable to the completion of this study.

References

BENNETT, M. J., COTTON, F. A. & WEAVER, D. L. (1966). *Nature, Lond.* **212**, 286.
BENNETT, M. J., COTTON, F. A., WEAVER, D. L., WILLIAMS, R. J. & WATSON, W. H. (1967). *Acta Cryst.* In the press.
COTTON, F. A. & ELDER, R. C. (1964). *Inorg. Chem.* **3**, 397.
COTTON, F. A. & FRANCIS, R. (1960). *J. Amer. Chem. Soc.* **82**, 2986.
COTTON, F. A., FRANCIS, R. & HORROCKS, W. D., JR. (1960). *J. Phys. Chem.* **64**, 1534.
FRANCIS, R. (1964). Ph.D. Thesis, Massachusetts Institute of Technology.
FRANCIS, R. & COTTON, F. A. (1961). *J. Chem. Soc.* p. 2078.
LIND, M. D., HAMOR, M. J., HAMOR, T. A. & HOARD, J. L. (1964). *Inorg. Chem.* **3**, 34.
MCGANDY, E. L. (1961). Ph.D. dissertation, Boston University. See also *Abstr. ACA Meeting, Boulder, Colorado* (1961), Abstr. No. 12.
THOMAS, R., SHOEMAKER, C. B. & ERIKS, L. (1966). *Acta Cryst.* **21**, 12.
VISWAMITRA, M. A. & KANNAN, K. K. (1960). *Nature, Lond.* **209**, 1016.
WELLS, A. F. (1962). *Structural Inorganic Chemistry*, 3rd ed. p. 998. London: Oxford Univ. Press.
ZASLOW, B. & RUNDLE, R. E. (1957). *J. Phys. Chem.* **61**, 490.

Acta Cryst. (1967). **23**, 586

The Crystal Structure of the Intermetallic Compound Cu_4Cd_3*

BY STEN SAMSON

Gates and Crellin Laboratories of Chemistry, California Institute of Technology, Pasadena, California 91109, *U.S.A.*

(*Received* 14 *December* 1966)

A determination of the crystal structure of the intermetallic compound Cu_4Cd_3 has been carried out with the use of packing maps [Samson, *Acta Cryst.* (1964), **17**, 491]. The structure has been refined by three-dimensional, least-squares techniques employing intensity data of 2537 reflections. The crystals are cubic, space group $F\bar{4}3m$ (T_d^2), with $a_0 = 25{\cdot}871 \pm 0{\cdot}002$ Å. There are 1124 atoms in the unit cell, distributed among 29 crystallographically different positions. The unit cube contains 568 icosahedra, 288 pentagonal prisms, 144 polyhedra of ligancy 15 (μ-phase polyhedra), and 124 Friauf polyhedra. Evidence has been found for a small degree of substitutional disorder.

The structure comprises two different substructures that interpenetrate, and each one is of considerable complexity. Each substructure represents a diamond-like arrangement, in one case of Friauf polyhedra, in the other case of icosahedra.

Introduction

The existence of the intermetallic compound Cu_4Cd_3 was established by Jenkins & Hanson (1924); the compound does not form on solidification of the melt but appears only after prolonged annealing at 450 to 500 °C through a reaction of a metastable eutectic mixture of the two phases, Cu_2Cd and Cu_5Cd_8, that always seem to be precipitated first.

Laves & Möller (1938) concluded from observation of powder patterns that Cu_4Cd_3 is isomorphous with β-Mg_2Al_3, which later was found by Perlitz (1944, 1946) to be cubic, space group $Fd3m$ (O_h^7), with approximately 1166 atoms per unit cube of edge $a_0 = 28{\cdot}22$ Å. A compound with structure apparently similar to those of Cu_4Cd_3 and β-Mg_2Al_3 is $NaCd_2$, which has a cubic unit cell of edge $a = 30{\cdot}56$ Å, space group $Fd3m$.

* Contribution 3459 from the Gates and Crellin Laboratories of Chemistry. The work reported in this paper was supported by Grant GP-4237 from the National Science Foundation.

A fairly detailed but incomplete picture of the structure of $NaCd_2$ was given by Samson (1962) and a detailed description of the structure of β-Mg_2Al_3 was published recently (Samson, 1965). In the latter paper brief mention was made of a single-crystal study of Cu_4Cd_3, which revealed a cubic structure, probable space groups $F\bar{4}3m$ (T_d^2), $F432$ (O^3), or $Fm3m$ (O_h^5), with approximately 1116 atoms per unit cube of edge $a_0=25{\cdot}87$ Å.

Dey & Quader (1965) show a list of powder data, which they obtained partly from photographs and partly from diffractometer scans of a sample, which they believed represented the pure phase Cu_4Cd_3. Each reflection in that list is indexed and there is excellent agreement between all the measured $\sin^2\theta$ values and those calculated for a tetragonal unit with $a_0=13{\cdot}701$ Å, $c_0=9{\cdot}944$ Å, and space group $P4_2/ncm$. Their sample was annealed for several days at 470 °C and had a measured density of 9·09 g.cm^{-3}.

Experimental

Sample preparation, composition, and density

Pieces of copper and cadmium of 99·9% purity were melted together in proportions corresponding to Cu_2Cd, Cu_4Cd_3, Cu_5Cd_8, and $CuCd_3$, the four known phases, and also in intermediate proportions. Each preparation was done in an alundum thimble that was heated inside a resistance furnace under dried argon gas at atmospheric pressure. Each melt was vigorously stirred and then cast into a cylindrical, water-cooled, copper mold.

Of Cu_4Cd_3, two cylindrical ingots were cast of about 150 g each and $\frac{1}{4}$ inch in diameter. These were sectioned into several rods. With one exception, each was sealed in an evacuated Pyrex tube and heat treated. The gradual conversion of the metastable eutectic, consisting of Cu_2Cd and Cu_5Cd_8, into the desired phase Cu_4Cd_3 was observed by comparing X-ray diffractometer scans of powder samples taken from the ingots after various periods of annealing.

The unannealed sample gave diffraction patterns of both Cu_2Cd and Cu_5Cd_8 but none of the intermediate phase. Samples annealed up to 660 hours at 490 °C contained the intermediate phase Cu_4Cd_3 but also small amounts of the other two phases. Continuation of the annealing of one sample to 990 hours at the same temperature resulted in apparently complete disappearance of the eutectic mixture, and after 2740 hours a tiny, needle-shaped crystal of about 10 to 15 microns in diameter was all that could be found for single-crystal X-ray work. This crystal was too small to be useful for the measurement of any but the strongest reflections.

Another sample was subsequently annealed for 1680 hours; this time the temperature was varied very slowly up and down between about 520 °C and slightly above the melting point (547 °C). Several irregular pieces up to about 1 mm in size, selected from the crushed alloy, were found to be single crystals of the desired phase. These were ground to spheres (Bond, 1951) and used for the single-crystal study. An X-ray powder study revealed that this sample represented, at least very nearly, a single phase.

The two alloys were chemically analyzed at a commercial laboratory. The results were as follows:

1. (2740 hours) Cu 43·30%, Cd 56·50%; *i.e.* $Cu_4Cd_{2.95}$
2. (1680 hours) Cu 43·80%, Cd 56·03%; *i.e.* $Cu_4Cd_{2.89}$

The density of the first alloy was determined in the same way as described earlier (Samson, 1965). Five independent measurements gave $\varrho_m=9{\cdot}10\pm0{\cdot}06$ g cm^{-3}, which is in accord with Dey & Quader's (1965) result.

In a recent paper on copper-cadmium alloys, Borg (1961) reported that a chemical analysis of a 'pure-phase' sample gave $43{\cdot}78\pm0{\cdot}03$ at.% Cd (which corresponds to $Cu_4Cd_{3.11}$), but, in the same paragraph, he states that the phase is slightly copper rich with respect to the formula Cu_4Cd_3. This contradiction, as well as the very close correspondence of his figure to the weight percentage of copper given in (2) above, indicates that a typographical error occurred here; furthermore, the component actually determined in Borg's analysis was copper and not cadmium. The latter component was determined by weight difference.

Unit cell and space group

Laue, rotation, and Weissenberg photographs of layer lines 0 to 5 about [011], obtained with the use of several single crystals, showed that the structure was face-centered cubic having Laue symmetry $m3m$. Only reflections of the type

$$hkl: h+k,\ k+l,\ (l+h)=2n$$

were present. The probable space group is, accordingly, $F432$, $Fm3m$, or $F\bar{4}3m$.

The length of the cube edge was determined from a photograph taken in a locally built, precision Weissenberg camera of 10 cm diameter with the film placed in the asymmetric position. Nickel-filtered Cu $K\alpha$ radiation was used ($\lambda_{\alpha1}=1{\cdot}54050$ Å, $\lambda_{\alpha2}=1{\cdot}54434$ Å). No functional dependence between a and θ was detectable in the reflection range $54°\leq\theta\leq79°$ used. The length of the cube edge was found to be $a_0=25{\cdot}871\pm0{\cdot}002$ Å. The chemical analyses and measured density indicate that the unit cube contains between 1120 and 1130 atoms.

A note on the paper by Dey & Quader

Since the powder data published by Dey & Quader (1965) were inconsistent with the results obtained here, a reexamination of numerous samples was carried out.

This time, a Guinier–Hägg camera of 40 mm radius was used. This camera employs a focusing crystal monochromator (Cu $K\alpha$ radiation) and a rotating, flat, powder-sample holder; it operates in vacuum and has a reflection range of $2°\leq\theta\leq42°$. The extreme

sharpness of the powder lines obtained with this camera results in high resolution even at low diffraction angles. The background is very low and permits accurate measurements of weak lines as well as detection of small amounts of phases accompanying the main ones.

The hexagonal structure [probably $C36$ type (doubled c axis)] reported for Cu_2Cd by Borg (1961), the cubic $D8_2$-type structure (γ-brass) reported for Cu_5Cd_8 (Owen & Pickup, 1933), and the hexagonal structure reported for $CuCd_3$ by Borg (1961) and Dey & Quader (1963) were confirmed. Kripyakevich, Gladyshevskii & Cherkashin (1952) said that Cu_2Cd crystallizes with the $C14$-type structure. It should be noted that most of the (extra) powder lines that account for the doubled c axis of Cu_2Cd can be indexed also on the basis of a body-centered cube of the γ-brass type (Cu_5Cd_8); therefore, caution is necessary to avoid confusion.

The lengths of the cell edges obtained here deviated very slightly from those given by Borg (1961), but are presumably less accurate since only the low-angle reflections were recorded (see above).

A complete list of reflections obtained from a 200-mesh powder of the sample of composition $Cu_4Cd_{2.89}$ that was annealed for 1680 hours (see sample preparation) is given in Table 1, where it is compared with the list of Dey & Quader (1965). It is seen that every powder line of the present sample is accounted for and that minute amounts of the Cu_5Cd_8 phase, probably a small fraction of 1%, are present. These are not detectable on conventional powder photographs. The indexing was done on the basis of $a_0=25{\cdot}871$ Å for Cu_4Cd_3 and $a_0=9{\cdot}55$ Å for Cu_5Cd_8 (γ-brass type) which has a considerable range of homogeneity and variable cell edge. The film was calibrated with potassium chloride [$a_0=6{\cdot}29294$ Å, Hambling (1953)].

Although there is suggestive agreement between the two powder patterns, sixteen lines in Dey & Quader's list cannot be accounted for on the basis of any of the four known copper-cadmium phases, and six medium-to-strong lines that are well resolved on the Guinier photograph are missing in their list. Powder photographs of samples of intermediate compositions failed to reveal the existence of a fifth phase.

It is possible that the unexplained reflections in Dey & Quader's list originate from oxides, but this possibility was not explored. The Guinier photograph of the sample $Cu_4Cd_{2.95}$ looked the same as that described above but was not evaluated quantitatively. Although the actual composition of the crystals used in this investigation cannot be determined with accuracy, the name Cu_4Cd_3 commonly used in the literature will be retained.

Intensity data

Intensities were measured on a Datex-automated, General Electric XRD 5 diffractometer, equipped with the one-quarter circle Goniostat, a scintillation counter modified according to Samson (1966), and a Nuclear-Chicago counter circuitry with pulse-height discriminator. The diffractometer was aligned according to Samson (1967*a*).

The crystal used was a sphere of 0·050 mm radius. Zirconium-filtered molybdenum radiation was necessary, otherwise undesirable absorption effects would have been caused by small irregularities in the sphere. Spherical absorption correction factors for $\mu R=1{\cdot}72$ were applied to the measured intensities.

The $2\theta:\theta$-scan method was used throughout at a scanning speed of 1° per minute. For each reflection the background was determined on either side of the peak from the number of counts accumulated in 100 seconds. Almost every reflection of magnitude F(obs) ≤ 150 (Table 3) is extremely weak, and the F(obs) value given is the weighted average of five or more non-consecutive measurements. The 2537 F(obs) values given in Table 3 were obtained from 12000 measurements ($2\theta_{max}=80°$), and there are 378 reflections with zero intensity.

Derivation of the trial structure

The trial structure was derived by the method outlined by Samson (1964), which employs *packing maps* and transparent templates of the kind shown in Fig. 1. The most important arguments that led to the solution of this structure are as follows:

1. *Fundamental structural principles*

(*a*) Previous crystal-structure studies of $Mg_3Cr_2Al_{18}$, $ZrZn_{22}$, $NaCd_2$, β-Mg_2Al_3 (Samson, 1958, 1961, 1962, 1965), and $Mg_{32}(Al, Zn)_{49}$ (Bergman, Waugh & Pauling 1957) led to the assumption that the dominant coordination shells in Cu_4Cd_3 are Friauf polyhedra and icosahedra. The Friauf polyhedron consists of two parts: a truncated (negative) tetrahedron bounded by four triangles and four hexagons and a regular (positive) tetrahedron which has its vertices out from the centers of the four hexagons.

(*b*) Truncated tetrahedra tend to join together to form layers, rows, or infinite, three-dimensional close packing or frameworks of Friauf polyhedra by sharing hexagons in most cases [in one case, hexagons and triangles ($Mg_{17}Al_{12}$, α-Mn)]; the occurrence of isolated Friauf polyhedra is rare (Samson, 1967*b*).

(*c*) If Friauf polyhedra do occur in a very complex cubic structure, they most likely will form a continuous, three-dimensional framework.

(*d*) The atoms at the vertices of any polyhedron are, in turn, surrounded by coordination shells that penetrate each other and the central one, and each of these atoms tends to enforce its own coordination requirements. This usually results in distortions of the polyhedra, which sometimes become considerable.

(*e*) In each case, where nonisolated Friauf polyhedra occur, each truncated tetrahedron is penetrated most often by twelve icosahedra and sometimes by nine icosahedra and three coordination shells of ligancy 13

Table 1. *Powder-diffraction data for* Cu_4Cd_3

Columns 1 and 2: data as presented by Dey & Quader (1965). Columns 3 to 6: data obtained in the present work. Alloy of composition $Cu_4Cd_{2.89}$ annealed for 1680 hours; see text. Crystal-monochromatized copper radiation, Guinier–Hägg camera of 40 mm radius. Asterisk indicates reflection from the Cu_5Cd_8 phase (γ-brass type), which is present in minute amounts, probably $<1\%$. Double asterisks (**) indicate reflections from both Cu_5Cd_8 and Cu_4Cd_3. All other reflections in columns 3 to 6 originate from Cu_4Cd_3. *vvw* − = barely visible, *vvw* = very very weak, *vw* = very weak, *w* = weak, *m* = medium, *s* = strong, *vs* = very strong.

Dey & Quader		Present work				Dey & Quader		Present work			
I_{obs}	$\sin^2\theta_{obs}$	$\sin^2\theta_{obs}$	$\sin^2\theta_{calc}$	Σh^2	I_{obs}	I_{obs}	$\sin^2\theta_{obs}$	$\sin^2\theta_{obs}$	$\sin^2\theta_{calc}$	Σh^2	I_{obs}
2	0·0126	—	—	—		2	0·1812	—	—	—	
4	0·0235	—	—	—		3	0·1873	0·1876	0·1873 0·1882	211 212	*vvw*
2	0·0250	—	—	—			—	0·1916	0·1918	216	*vvw*
—		0·0283	0·0284	32	*vvw*−		—	0·1945	0·1945	219	*vvw*
4	0·0300	—	—	—			—	0·2023	0·2024	228	*vvw*
—		0·0310	0·0311	35	*vvw*−	3	0·2162	0·2155	0·2158	243	*w*
—		0·0319	0·0320	36	*vw*		—	0·2200	0·2202	248	*vw*
2	0·0366	—	—	—			—	0·2227	0·2229	251	*vw*
—		0·0381	0·0382	43	*vw*		—	0·2306	0·2309	260	*vw*
—		0·0390	0·0391	44	*vvw*		—	0·2341**	0·2344**	264**	*vw***
—		0·0453	0·0453	51	*vvw*	8	0·2372	0·2367	$0·2367\alpha_1$	267	*vw*
—		0·0496	0·0497	56	*vw*			0·2379	$0·2379\alpha_2$		
6	0·0525	0·0523	0·0524	59	*w*−	2	0·2443	0·2437	$0·2438\alpha_1$	275	*vvw*
3	0·0538	—	—	—				—	$0·2450\alpha_2$		
—		0·0568	0·0568	64	*w*−		—	0·2473*	$0·2473\alpha_1$*	38*	*vvw**
								—	$0·2486\alpha_2$		
2	0·0606	—	—	—			—	0·2510	$0·2509\alpha_1$	283	*vvw*
—		0·0637	0·0639	72	*vw*			—	$0·2521\alpha_2$		
6	0·0655	0·0652*	0·0652*	10*	*vvw**	8	0·2589	0·2588	$0·2588\alpha_1$	292	*vw*
—		0·0667	0·0666	75	*vw*			—	$0·2601\alpha_2$		
—		0·0673	0·0675	76	*w*	10	0·2637	0·2626	$0·2624\alpha_1$	296	*w*−
—		0·0736	0·0737	83	*m*			0·2638	$0·2637\alpha_2$		
10	0·0742	0·0745	0·0746	84	*w*		—	0·2651	$0·2650\alpha_1$	299	*vvw*
								—	$0·2663\alpha_2$		
—		0·0781**	0·0781**	88**	*w*+**		—	0·2718	$0·2721\alpha_1$	307	*vvw*
3	0·0806	0·0806	0·0808	91	*m*−			—	$0·2735\alpha_2$		
3	0·0853	0·0853	0·0852	96	*m*−		—	0·2733*	$0·2734\alpha_1$*	42*	*vvw**
25	0·0879	0·0877	0·0879	99	*s*			—	$0·2748\alpha_2$		
—		0·0888	0·0888	100	*vw*	10	0·2878	0·2865**	$0·2863\alpha_1$**	323**	*m***
								0·2880	$0·2877\alpha_2$		
—		0·0912*	0·0913*	14*	*vvw**		—	0·2909	$0·2907\alpha_1$	328	*vw*
—		0·0922	0·0923	104	*s*−			0·2924	$0·2922\alpha_2$		
12	0·0950	0·0949	0·0950	107	*s*−		—	—	—	—	
10	0·0962	0·0958	0·0959	108	*m*	8	0·3014	0·3051	$0·3049\alpha_1$	344	*vvw*
10	0·1022	0·1020	0·1021	115	*m*		—	0·3070	$0·3065\alpha_2$		
—		0·1042*	0·1043*	16*	*vvw**		—	0·3127*	$0·3124\alpha_1$*	48*	*vvw**
—		0·1066	0·1066	120	*w*			—	$0·3140\alpha_2$		
—		0·1092	0·1092	123	*w*−	35	0·3158	0·3157	$0·3156\alpha_1$	356	*s*−
65	0·1138	0·1136	0·1137	128	*vs*			0·3174	$0·3171\alpha_2$		
							—	0·3190	$0·3191\alpha_1$	360	*vvw*
—		0·1164	0·1163	131	*s*			—	$0·3207\alpha_2$		
40	0·1173	0·1172**	0·1172**	132**	*s***	28	0·3220	0·3219	$0·3128\alpha_1$	363	*m*−
—		0·1208	0·1208	136	*m*			0·3236	$0·3234\alpha_2$		
—		0·1233	0·1234	139	*vs*		—	0·3255*	$0·3255\alpha_1$*	50*	*vvw**
100	0·1244	0·1242	0·1243	140	*vw*			0·3272*	$0·3271\alpha_2$*		
—		0·1278	0·1279	144	*vw*	3	0·3339	0·3334	$0·3333\alpha_1$	376	*vw*
								—	$0·3349\alpha_2$		
50	0·1311	0·1305**	0·1305**	147**	*s***	10	0·3430	0·3406	$0·3404\alpha_1$	384	*w*
25	0·1355	0·1351	0·1350	152	*s*			0·3423	$0·3421\alpha_2$		
—		0·1377	0·1376	155	*vvw*	25	0·3496	0·3477	$0·3475\alpha_1$	392	*s*
—		0·1419	0·1421	160	*vvw*			0·3497	$0·3492\alpha_2$		
—		0·1435*	0·1434*	22*	*w**		—	0·3504	$0·3501\alpha_1$	395	*m*
—		0·1447	0·1447	163	*m*			0·3523**	$0·3519\alpha_2$**		
20	0·1452	0·1457	0·1456	164	*m*	8	0·3655	0·3649	$0·3643\alpha_1$	411	*w*
								0·3667	$0·3661\alpha_2$		
—		0·1490	0·1492	168	*vvw*	2	0·3717	0·3715	$0·3714\alpha_1$	419	*vvw*
20	0·1524	0·1517	0·1518	171	*m*+			0·3735	$0·3732\alpha_2$		

Table 1 (*cont.*)

Dey & Quader		Present work				Dey & Quader		Present work			
I_{obs}	$\sin^2\theta_{obs}$	$\sin^2\theta_{obs}$	$\sin^2\theta_{calc}$	Σh^2	I_{obs}	I_{obs}	$\sin^2\theta_{obs}$	$\sin^2\theta_{obs}$	$\sin^2\theta_{calc}$	Σh^2	I_{obs}
5	0·1572	0·1561**	0·1563**	176**	*m*—**	2	0·3798	—	—	—	
3	0·1594	0·1589	0·1589	179	*vw*	2	0·3835	—	—	—	
5	0·1650	—	—	—		15	0·4005	0·4003	$0{\cdot}3998\alpha_1$	451	*m*
								0·4025	$0{\cdot}4018\alpha_2$		
	—	0·1662	0·1660	187	*vvw*	2	0·4183	0·4190	$0{\cdot}4181\alpha_1$	472	*vvw*
5	0·1703	—	—	—				—	$0{\cdot}4204\alpha_2$	—	
	—	0·1778	0·1776	200	*vw*	2	0·4209	—	—	—	
8	0·1803	—	—	—		2	0·4295	—	—	—	

or 14, or ten icosahedra and two coordination shells of *L*13 or *L*14.

(*f*) In infinite, three-dimensional frameworks of Friauf polyhedra each hexagon of a truncated tetrahedron, not shared by another truncated tetrahedron, is usually shared by a hexagonal antiprism that has two atoms at the extended poles (*L*14) or by a μ-phase polyhedron, the *L*15 shell observed in the μ-phase W_6Fe_7 (Arnfelt & Westgren, 1935); see also Samson (1967*b*).

The hexagonal antiprisms and the μ-phase polyhedra often terminate groupings of Friauf polyhedra.

(*g*) Truncated tetrahedra have (so far) never been observed to penetrate one another. This is part of the reason why they seem to dominate in most structures although they are by far outnumbered by other kinds of coordination shells, especially by icosahedra. The Friauf-polyhedra framework, therefore, comprises in most cases the dominant number of crystallographically different positions and represents the most favorable starting point in the search for a trial structure in which it is anticipated.

(*h*) The metrical nature of the icosahedron requires that the average size of the contiguous spheres at the vertices be nearly 1·10 times that of the central sphere. Since structures incorporating Friauf polyhedra (and icosahedra) usually contain atoms differing in radius by significantly more than ten per cent (exceptions α-Mn and α-VAl_{10}), each icosahedral coordination shell has, in almost all cases, about half its vertices occupied by large atoms and the other half by small atoms.

(*i*) The distribution of atoms of different sizes at the vertices of the icosahedron causes deformation.

(*j*) It does not seem possible to build a space-filling structure in which each atom is surrounded by an icosahedral coordination shell. In such a case, a central icosahedron must be penetrated by twelve others, and each of these in turn by twelve *etc.*, each center atom now being about ten per cent smaller than the atoms at the vertices. In any known structure, the icosahedra are associated with other kinds of coordination shells by interpenetration or by sharing their triangles.

(*k*) Hexagonal antiprisms are more frequently observed in metallic structures than are hexagonal prisms. While the later give rise to octahedral interstices, the former produce tetrahedral ones, thus reducing the amount of interstitial space.

(*l*) The Friauf polyhedron, the μ-phase polyhedron, and the hexagonal antiprism are related to one another as follows: The Friauf polyhedron can be described as a hexagonal antiprism consisting of a large and a small hexagon; out from the center of the small hexagon is one atom and out from the larger hexagon are three atoms forming a triangle. The μ-phase polyhedron is obtained through replacement of these three atoms by two atoms. The coordination shells of ligancy 14 are

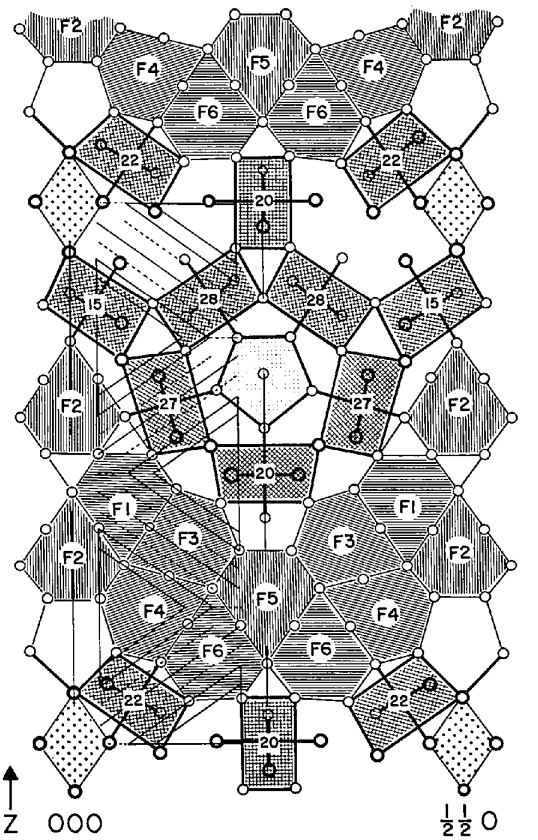

Fig. 1. Packing map of the structure of Cu_4Cd_3 representing the 'most useful plane' [(110) plane] for space group $F\bar{4}3m$. Many of the plus-minus atoms are omitted for the sake of perspicuity. The polygons *F*1–6 are sections through Friauf polyhedra. The sections marked 15, 20, 22, 27, and 28 (ID numbers; see Table 4) represent icosahedra. There are, furthermore, four octahedra (dotted) and one pentagonal prism (slightly above center). The origin of the cube coincides with the center of the lower left octahedron.

often hexagonal antiprisms, each one with two atoms at the extended poles.

(*m*) The icosahedron can be described as a pentagonal antiprism, which has two atoms at the extended poles. It thus provides a condition favorable for the formation of tetrahedral interstices.

2. *Geometrical arguments* (*packing maps*)

An understanding of the following arguments and terminology requires familiarity with the previous paper (Samson, 1964), which is extremely brief. If a more detailed description is required, it will have to be given elsewhere.

(*a*) The space groups $F432$ and $Fm3m$ have two *most useful planes* each, the (100) and (110) planes. Space group $F\bar{4}3m$ has a single *most useful plane*, the (110) plane. Any space-filling structure of this space group can be completely surveyed and described with a single packing map of this plane, irrespective of the size of the unit cell.

(*b*) Exploration of the packing maps with transparent templates of the kind $F1$–6 (Fig. 1), representing polygonal sections of Friauf polyhedra, leads to a rapid exclusion of all but space group $F\bar{4}3m$ if the conditions described in 1(*c*) and (*g*) above are to be fulfilled, even if allowance is made for distortions according to 1(*d*).

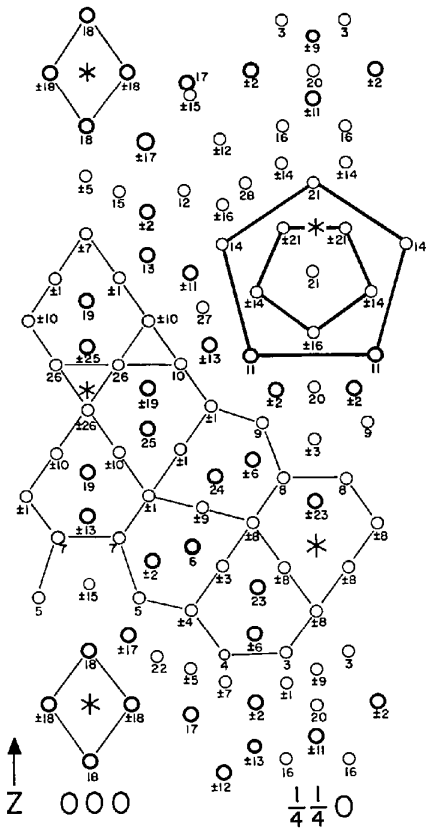

Fig. 2. Auxiliary map for the identification of the crystallographically different atoms on the packing map. The number near each circle represents the same atom number as in Table 2. Heavy circles: Cd; light circles: Cu.

(*c*) The positioning of the polygonal sections $F1$–6 as shown in Fig. 1, is the only one that corresponds to condition 1(*c*) and simultaneously satisfies the symmetry requirements exhibited on the packing map. To avoid making the picture too complex not all the necessary lines are drawn out in Fig. 1. The actual map used is shown in Fig. 5 of the previous paper (Samson, 1964).

The perfect geometrical fit between the sets of the six polygonal sections $F1$–6 and the packing map arouses confidence as to the correctness of this part (about 50%) of the structure.

(*d*) Additional polygonal sections of type F can be placed only in areas where they would represent Friauf polyhedra that are isolated from the framework. Such a situation seems unlikely at this stage: refer 1(*b*).

(*e*) The remaining area on the packing map is now explored with polygonal sections of icosahedra, in accordance with 1(*e*) and 1(*j*) above, and allowance is made for the deformations according to 1(*d*), 1(*h*), and 1(*i*). Note that the argument 1(*e*) above is the most important one in the search for a meaningful structural motive that is compatible with the one represented by the polygonal sections $F1$–6.

(*f*) The positioning of the sections of the icosahedra marked 15, 20, 22, 27, and 28 in Fig. 1 satisfies the symmetry requirements exhibited on the actual map used (not shown here) and corresponds to a continuous, three-dimensional framework of icosahedra that are interpenetrated by icosahedra as well as other kinds of coordination shells.

(*g*) Discs representing (110) sections through the spheres outlining the domains of neighbors that must not overlap can now be placed so as to cover the areas of the packing map that are not covered by the polygonal sections. It is then seen that a very satisfactory space filling is achieved with a minimum of interstitial space and no void anywhere in the structure.

(*h*) Each kind of polyhedron present in the structure can now be traced out on the packing map, and it is seen that the rules oulined in 1(*f*), 1(*g*), and 1(*k*) also apply to this trial structure. With the atoms placed to fit the argument 1(*h*), and, furthermore, to fit the assumption that the large atoms (cadmium) require higher coordination numbers than the small ones (copper), the unit cell contains one formula unit of $Cu_{640}Cd_{484}$, which corresponds to the composition $Cu_4Cd_{3.03}$ and a calculated density of $\varrho = 9{\cdot}115$ g.cm^{-3}. This result agrees well with the experimental values given under *Sample preparation*.

For the well-trained user of the packing map it is possible to form an almost complete, three-dimensional mental picture of the structure and to study every structural detail with the aid of Figs. 1 and 2. Each atomic positional parameter is obtained from the map. The number near each small circle in Fig. 2 represents the same atom number as in Table 2; there are 29 crystallographically different atoms. A number of 'plus-

minus' atoms have been omitted from Fig. 1 to decrease the complexity of the picture, but these are included in Fig. 2.

Refinement of the structure

With the 1124 atoms placed in the 29 different positions given in Table 2 a very promising agreement between observed and calculated structure factors was obtained.

The 47 positional parameters, the 29 isotropic temperature factors, and the scale factor were refined by full-matrix (77×77), least-squares calculations on the Institute's IBM 7040-7094 crystallographic computing system CRYRM (Duchamp, 1964). The cubic space groups are treated in this program as outlined by Webb (1964). The scattering factors listed in Table 3.3. 1B of *International Tables for X-ray Crystallography* (1962) were employed, corrected for anomalous dispersion (real part only) according to Dauben & Templeton (1955). The 2537 measured data, of which 378 were of zero intensity, were used with weights assigned according to Peterson & Levy (1957); the reflections with zero intensity were given zero weight. The quantity minimized was $\Sigma\omega(F_o^2-F_c^2)^2$; full shifts were used throughout.

The rapidity of convergence is hard to evaluate because of an initial error in the program that caused exaggerated shifts for some of the parameters of atoms in special positions; the R value was oscillating between about 0·13 and 0·17. After correction of this error, convergence was achieved with three more cycles for each of the following three experiments:

(1) In the initial model the atoms 12 and 16 (Table 2) were assumed to be cadmium and 14 and 15 to be copper. The resulting 'thermal parameters', in this case more properly called B values, were $B(12)=1{\cdot}91$, $B(16)=2{\cdot}52$, $B(14)=0{\cdot}68$, and $B(15)=0{\cdot}82$ and aroused suspicion of substitutional disorder. The R index $\Sigma\,||F_o|-|F_c||/\Sigma|F_o|$ was 0·132 and the goodness of fit $\Sigma\omega(F_o^2-F_c^2)^2/(m-s)$ was 2·22.

(2) To account approximately for the substitutional disorder, the copper and cadmium atoms were apportioned to the four point sets in accordance with Table 2, which also gives the resulting B values. The R value was 0·128 and the goodness of fit was 1·77.

(3) Inclusion of the four population factors and an additional one for atom no. 22 in the now 82×82 full matrix gave the following result:

Atom no.	% Cd	% Cu	B (Å²)
12	81 ± 3	19 ± 3	1·46
14	64 ± 3	36 ± 3	2·16
15	14 ± 3	86 ± 3	1·29
16	76 ± 3	24 ± 3	2·11
22	5 ± 5	95 ± 5	0·85

The R value was 0·127 and the goodness of fit was 1·65.

The positional parameters for the last two cases came out to be practically identical, while in the first

Table 2. *The final positional parameters and isotropic temperature factors for assumed composition* $Cu_{640}Cd_{484}$.

The substitutional disorder in positions 12, 14, 15, and 16 is approximate.

Atom No.	Kind	Point set	x	y	z	B
1	Cu	96(*i*) *xyz, etc.*	0·1018 (1)	0·1714 (1)	0·4662 (1)	1·16 (5) Å²
2	Cd	96(*i*) *xyz, etc.*	0·0036 (1)	0·1362 (1)	0·2256 (1)	1·22 (3)
3	Cu		0·2142 (2)		0·0813 (2)	1·15 (7)
4	Cu		0·1476 (2)		0·0784 (2)	1·19 (8)
5	Cu		0·0560 (2)		0·1683 (2)	1·11 (6)
6	Cd		0·1138 (1)		0·2499 (1)	1·06 (4)
7	Cu		0·0339 (2)		0·2604 (2)	1·28 (8)
8	Cu		0·2157 (2)		0·3517 (2)	1·27 (8)
9	Cu		0·1931 (2)		0·4424 (2)	1·18 (6)
10	Cu	48(*h*) *xxz, etc.*	0·1026 (2)		0·5335 (2)	1·03 (7)
11	Cd		0·1793 (1)		0·5474 (1)	1·22 (4)
12	~($\frac{2}{3}$Cd+$\frac{1}{3}$Cu)		0·1060 (1)		0·8117 (1)	1·22 (5)
13	Cd		0·0663 (1)		0·7043 (1)	1·24 (4)
14	~($\frac{1}{2}$Cu+$\frac{1}{2}$Cd)		0·1498 (1)		0·7244 (2)	1·87 (6)
15	~($\frac{2}{3}$Cu+$\frac{1}{3}$Cd)		0·0354 (2)		0·8091 (2)	1·86 (8)
16	~($\frac{1}{2}$Cu+$\frac{1}{2}$Cd)		0·2130 (2)		0·9138 (1)	1·59 (6)
17	Cd		0·1119 (1)		0·9796 (1)	1·16 (4)
18	Cd	24(*f*) *x*00, *etc.*	0·0876 (2)			1·21 (6)
19	Cd		0·3635 (2)			0·97 (5)
20	Cu	24(*g*) $x\frac{1}{4}\frac{1}{4}$, *etc.*	0·5006 (3)			1·27 (9)
21	Cu		0·6793 (3)			1·49 (11)
22	Cu		0·0744 (3)			0·69 (12)
23	Cd		0·1815 (3)			1·04 (7)
24	Cd		0·3632 (2)			1·13 (7)
25	Cd	16(*e*) *xxx, etc.*	0·4315 (2)			1·06 (7)
26	Cu		0·5346 (3)			1·28 (14)
27	Cu		0·6262 (3)			1·12 (12)
28	Cu		0·8203 (4)			0·98 (13)
29	Cd	4(*c*) $\frac{1}{4}\frac{1}{4}\frac{1}{4}$, *etc.*				1·04 (17)

case the x parameters for the atoms 5, 27, and 28 came out to be higher by almost exactly two standard deviations.

Because of the difference in size between the atoms of copper and cadmium, a substitutional disorder must be expected to cause displacements, not only of the nearest neighbors but also of atoms in successive shells. For this reason, it is extremely difficult to uncouple the effects of substitutional disorder (or partial occupancy) and thermal vibrations. The population factors obtained in case (3) result in the composition $Cu_{6.22}Cd_{5.02}$ or $Cu_4Cd_{3.23}$, which is inconsistent with the results given in the section on sample preparation, *etc.* The occupancies given in Table 2 correspond to the gross composition of the ordered model and are rough estimates.

The structural parameters used for all subsequent calculations are those given in Table 2. The structure factors are listed in Table 3 and the interatomic distances in Table 4. An electron density section representing the (110) plane passing through the origin of the cube is shown in Fig. 3.

The relatively high R value results from the extremely large number of very weak reflections, for which the standard deviations calculated on the basis of the counting statistics (column 3, Table 3) are also high. The goodness of fit reflects that the overall agreement is very reasonable.

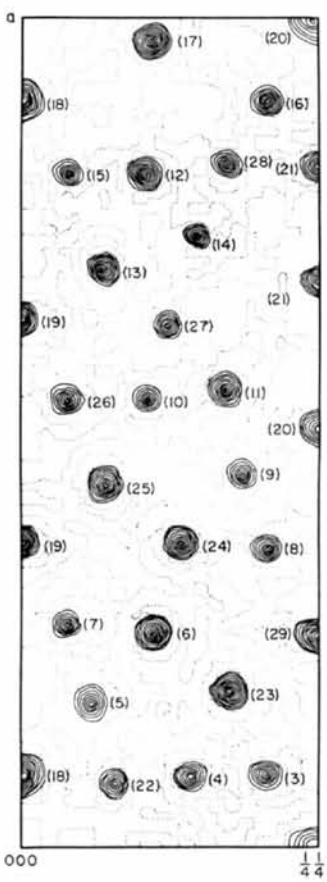

Fig. 3. An electron-density section representing the (110) plane passing through the origin of the cube. The number in parentheses near each peak is the atom number.

Description of the structure

The structure can be described most conveniently in terms of two kinds of infinite, three-dimensional framework that interpenetrate one another. Each framework represents a diamond-like arrangement, in one case of Friauf polyhedra, in the other case of icosahedra.

The diamond-like arrangement of Friauf polyhedra consists of the three types of complex shown in Fig. 4. The octahedron of T_d symmetry [Fig. 4(*a*)] comprises ten Friauf polyhedra, $4F1+6F2$; see packing map, Fig. 1. The tetrahedral arrangement shown in Fig. 4(*c*) consists of the Friauf polyhedra $F5+4F6$ (Fig. 1), and the dark polyhedra in Fig. 4(*b*) are $F3+3F4$. The cubic unit contains four octahedra [Fig. 4(*a*)] that are arranged about the points $\frac{1}{2}, \frac{1}{2}, \frac{1}{2}$; $\frac{1}{2}00$; $0\frac{1}{2}0$; $00\frac{1}{2}$ (point set 4(*b*) in $F\bar{4}3m$) and four tetrahedra [Fig. 4(*c*)] that are about the points $\frac{1}{4}, \frac{1}{4}, \frac{1}{4}$, *etc.* [point set 4(*c*)]. The layer of the dark Friauf polyhedra serves as a link between the octahedra and the tetrahedra. The infinite, three-dimensional framework of Friauf polyhedra thus formed is shown in Fig. 5. It is seen that the tetrahedra, the dark layers, and the octahedra alternate in a zigzag fashion.

The diamond-like arrangement of icosahedra may be described in terms of two kinds of complex. One of them is shown in Fig. 6. It is seen [Fig. 6(*a*)] that five icosahedra are arranged about an approximate fivefold axis of symmetry, thus enclosing a pentagonal prism. These icosahedra are the ones that have been marked 20, 27, and 28 on the packing map (Fig. 1). A set of six such fivefold rings are arranged at the vertices of an octahedron of T_d symmetry. All six rings interpenetrate and share icosahedra in such a way that the aggregate [Fig. 6(*c*)] consists of fourteen icosahedra that enclose six pentagonal prisms of the kind shown in Fig. 6(*a*). Fig. 6(*b*) shows two such fivefold rings interpenetrating at right angles. It is now seen that the pentagonal prism [in Fig. 6(*a*)] is shared between two icosahedra, one above and the other below the plane

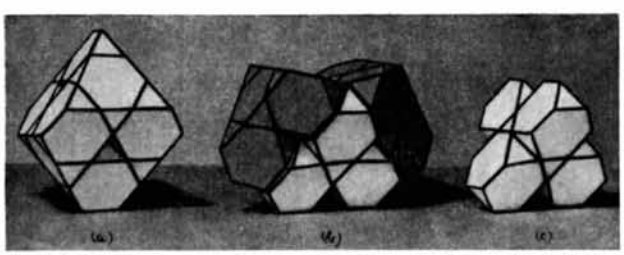

Fig. 4. The three types of atom complexes that form the infinite, three-dimensional framework of Friauf polyhedra shown in Fig. 5. (*a*) A complex of ten Friauf polyhedra, $4F1+6F2$ forming an octahedron of *Td* symmetry. (*b*) The dark Friauf polyhedra are $F3+3F4$. (*c*) This tetrahedron consists of $F5+4F6$ (compare with Fig. 1).

Table 3. *Observed and calculated structure factors*

Each group of four columns contains, from left to right, indices *l*, observed structure factors, standard deviations ($\sigma|F|$) according to Peterson & Levy (1957), and calculated structure factors. Three dashes in column 2 indicate that the weighted average of five or more measurements was negative or zero.

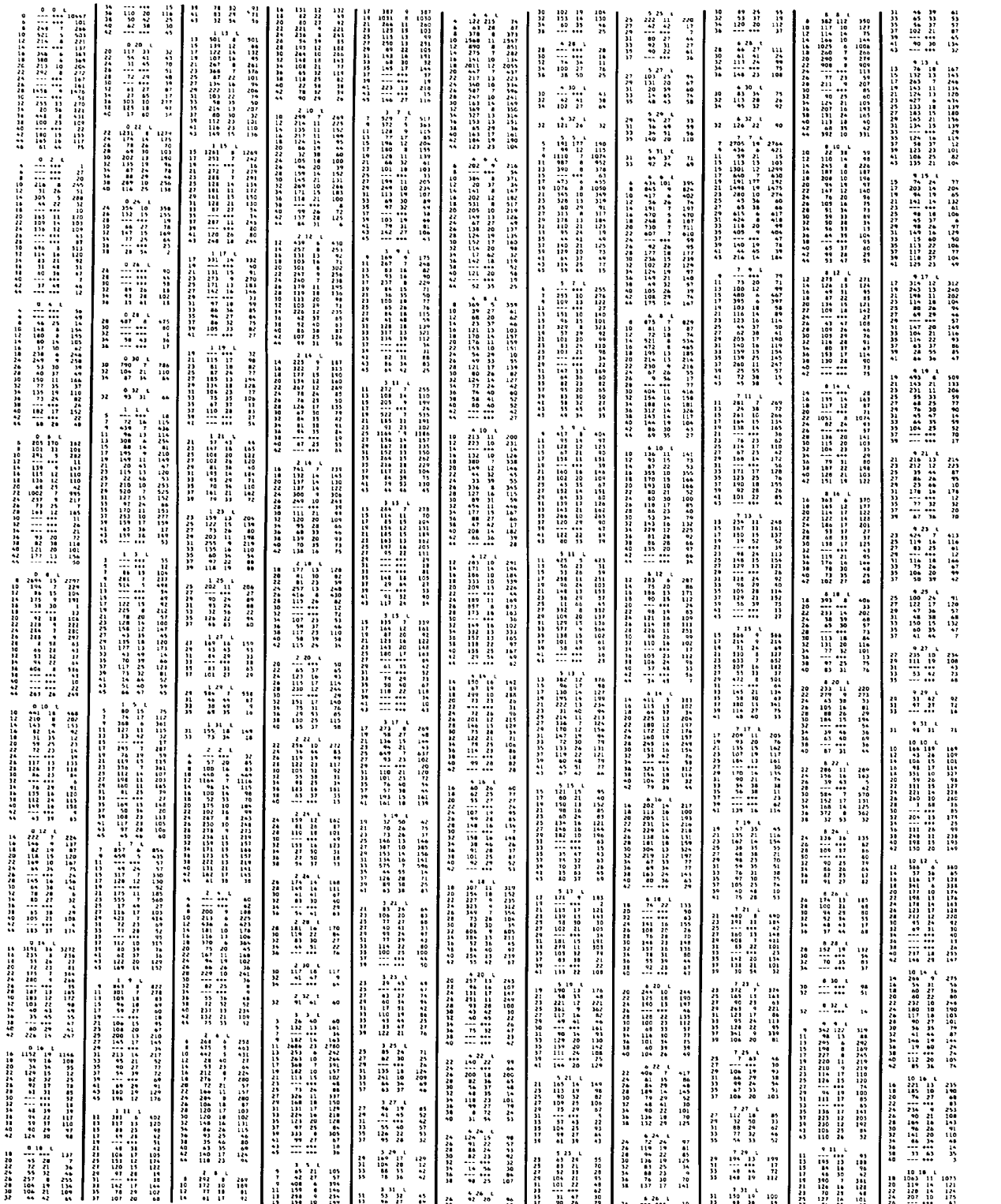

Table 3 (*cont.*)

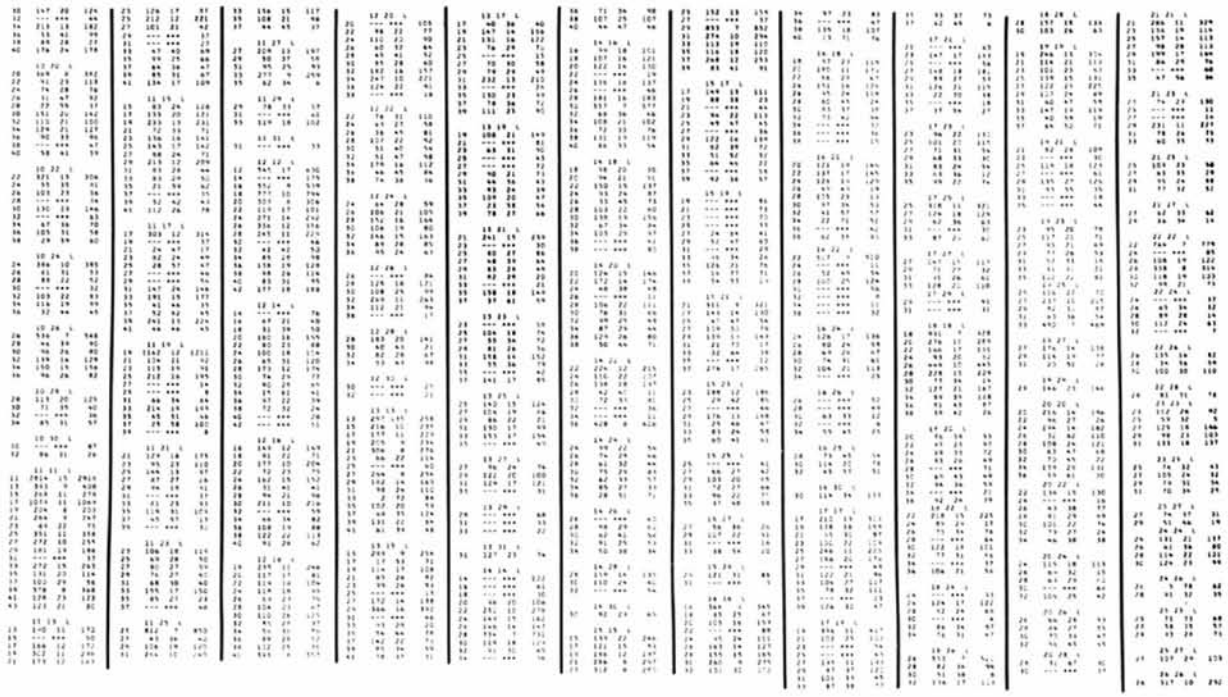

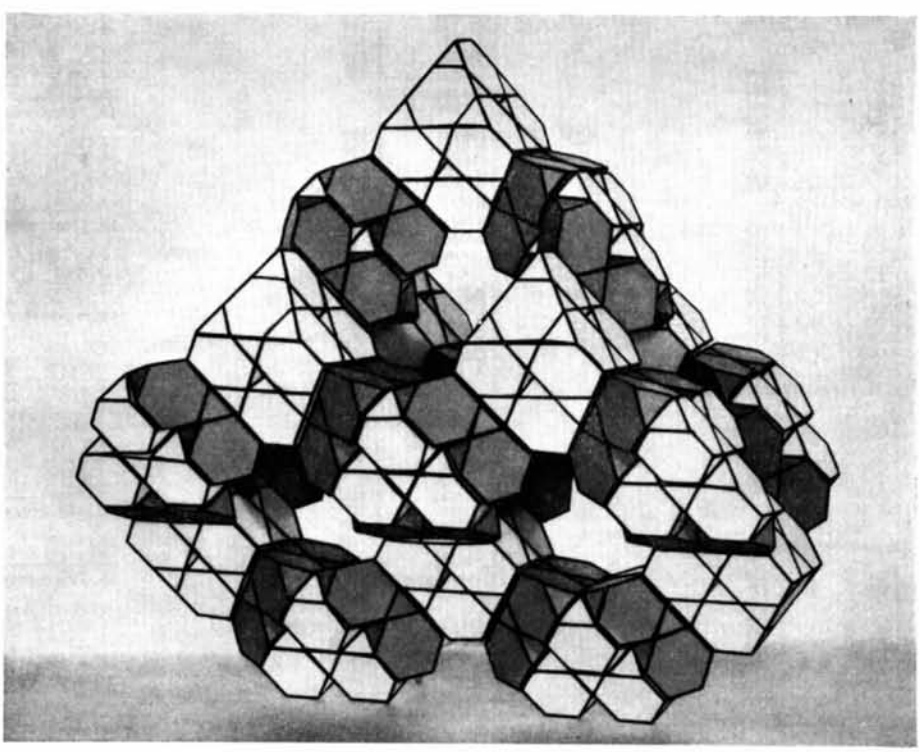

Fig. 5. The three atom complexes shown in Fig. 4(*a*), (*b*), and (*c*), form the infinite, three-dimensional framework of Friauf polyhedra shown here.

Table 4. *Interatomic distances*

An X in place of the chemical symbol indicates substitutional disorder between copper and cadmium. The number in parentheses following the name of a polyhedron is the identification number referred to as ID.

Kind of Atom	Ligancy	Distance Å
Cu(1)	1 Cu(1)	2.547
	1 Cu(1)	2.488
	1 Cd(2)	2.916
	1 Cd(6)	2.920
	1 Cu(7)	2.488
	1 Cu(9)	2.506
	1 Cu(10)	2.490
	1 Cd(11)	2.912
	1 Cd(13)	2.876
	1 Cd(19)	2.918
	1 Cd(24)	2.953
	1 Cd(25)	2.939
	12, icosahedron (1)	
Cd(2)	1 Cu(1)	2.916
	1 Cd(2)	3.272
	1 Cu(3)	2.864
	1 Cu(4)	2.812
	1 Cu(5)	2.888
	1 Cd(6)	2.976
	1 Cu(7)	2.902
	1 Cu(9)	2.923
	1 Cd(11)	3.006
	1 X (12)	3.095
	1 Cd(13)	3.135
	1 X (15)	2.936
	1 X (16)	3.075
	1 Cd(17)	3.073
	1 Cu(20)	3.013
	15, Hexagonal anti-prism + 3 (2)	
Cu(3)	2 Cd(2)	2.864
	1 Cu(3)	2.618
	1 Cu(4)	2.438
	2 Cd(6)	2.882
	2 Cu(8)	2.509
	2 Cu(9)	2.533
	1 Cu(20)	2.489
	1 Cd(23)	2.856
	12, icosahedron (3)	
Cu(4)	2 Cd(13)	2.812
	1 Cu(3)	2.438
	2 Cu(4)	2.531
	2 Cu(5)	2.498
	2 Cd(6)	2.933
	1 Cd(17)	2.872
	1 Cu(22)	2.679
	1 Cd(23)	2.939
	12, icosahedron (4)	
Cu(5)	2 Cd(2)	2.888
	2 Cu(4)	2.498
	1 Cd(6)	2.987
	1 Cu(7)	2.516
	2 X (15)	2.495
	2 Cd(17)	2.851
	1 Cd(18)	2.925
	1 Cu(22)	2.520
	12, icosahedron (5)	
Cd(6)	2 Cu(1)	2.920
	2 Cu(3)	2.882
	2 Cu(4)	2.933
	1 Cu(5)	2.987
	1 Cu(7)	2.934
	2 Cu(8)	2.921
	2 Cu(9)	2.915
	2 Cd(2)	2.976
	1 Cd(23)	3.043
	1 Cd(24)	3.051
	16, Friauf polyhedron F4	
Cu(7)	2 Cu(1)	2.488
	2 Cd(2)	2.902
	1 Cu(5)	2.516
	1 Cd(6)	2.934
	1 Cu(7)	2.484
	2 Cd(13)	2.874
	2 X (15)	2.541
	1 Cd(19)	2.942
	12, icosahedron (7)	
Cu(8)	2 Cu(3)	2.509
	2 Cd(6)	2.921
	1 Cu(8)	2.514
	2 Cu(8)	2.466
	1 Cu(9)	2.485
	2 Cd(23)	2.934
	1 Cd(24)	2.900
	1 Cd(29)	2.917
	12, icosahedron (8)	
Cu(9)	2 Cu(1)	2.506
	2 Cd(2)	2.923
	2 Cu(3)	2.533
	2 Cd(6)	2.915
	1 Cu(8)	2.485
	1 Cd(11)	2.765
	1 Cu(20)	2.569
	1 Cd(24)	2.905
	12, icosahedron (9)	
Cu(10)	2 Cu(1)	2.490
	2 Cu(10)	2.528
	1 Cd(11)	2.830
	2 Cd(13)	2.919
	2 Cd(19)	2.927
	1 Cd(25)	2.919
	1 Cu(26)	2.490
	1 Cu(27)	2.547
	12, icosahedron (10)	
Cd(11)	2 Cu(1)	2.912
	2 Cd(2)	3.006
	1 Cu(9)	2.765
	1 Cu(10)	2.830
	2 Cd(13)	3.034
	2 X (14)	2.992
	2 X (16)	3.087
	1 Cu(20)	2.856
	1 Cu(27)	2.817
	14, pentagonal prism +4 (11)	
X(12)	2 Cd(2)	3.095
	2 X (12)	3.012
	1 Cd(13)	3.135
	1 X (14)	2.770
	1 X (15)	2.582
	2 X (16)	2.887
	2 Cd(17)	2.973
	1 Cu(28)	2.707
	12, pentagonal prism +2 (12)	
Cd(13)	2 Cu(1)	2.876
	2 Cd(2)	3.135
	2 Cu(7)	2.874
	2 Cu(10)	2.919
	2 Cd(11)	3.034
	1 X (12)	3.135
	1 X (14)	3.098
	1 X (15)	2.937
	1 Cd(19)	2.993
	1 Cu(27)	2.981
	15, Hexagonal anti-prism + 3 (13)	
X(14)	2 Cd(11)	2.992
	1 X (12)	2.770
	1 Cd(13)	3.098
	2 X (14)	2.729
	2 X (16)	2.829
	2 Cu(21)	2.783
	1 Cu(27)	2.683
	1 Cu(28)	2.713
	12, pentagonal prism +2 (14)	
X(15)	2 Cd(2)	2.936
	2 Cu(5)	2.495
	2 Cu(7)	2.541
	1 X (12)	2.582
	1 Cd(13)	2.937
	1 X (15)	2.593
	2 Cd(17)	2.871
	1 Cd(18)	2.969
	12, icosahedron (15)	
X(16)	2 Cd(2)	3.075
	2 Cd(11)	3.087
	2 X (12)	2.887
	2 X (14)	2.829
	1 X (16)	2.709
	1 Cu(20)	2.597
	1 Cu(21)	2.762
	1 Cu(28)	2.708
	12, pentagonal prism +2 (16)	
Cd(17)	2 Cd(2)	3.073
	1 Cu(4)	2.872
	2 Cu(5)	2.851
	2 X (12)	2.973
	2 X (15)	2.871
	2 Cd(17)	3.347
	2 Cd(18)	3.008
	1 Cu(22)	2.809
	14, pentagonal prism +4 (17)	
Cd(18)	2 Cu(5)	2.925
	2 X (15)	2.969
	4 Cd(17)	3.008
	4 Cd(18)	3.206
	2 Cu(22)	2.745
	14, pentagonal prism +4 (18)	
Cd(19)	4 Cu(1)	2.918
	2 Cu(7)	2.942
	4 Cu(10)	2.927
	2 Cu(26)	2.924
	2 Cd(13)	2.993
	2 Cd(25)	3.062
	16, Friauf polyhedron F2	
Cu(20)	4 Cd(2)	3.013
	2 Cu(3)	2.489
	2 Cu(9)	2.569
	2 Cd(11)	2.856
	2 X (16)	2.597
	12, icosahedron (20)	
Cu(21)	4 X (14)	2.783
	2 X (16)	2.762
	4 Cu(21)	2.587
	2 Cu(28)	2.571
	12, pentagonal prism +2 (21)	
Cu(22)	3 Cu(4)	2.679
	3 Cu(5)	2.520
	3 Cd(17)	2.809
	3 Cd(18)	2.745
	12, icosahedron (22)	
Cd(23)	3 Cu(3)	2.856
	3 Cu(4)	2.939
	6 Cu(8)	2.934
	3 Cd(6)	3.043
	1 Cd(29)	3.072
	16, Friauf polyhedron F6	
Cd(24)	6 Cu(1)	2.953
	3 Cu(8)	2.900
	3 Cu(9)	2.905
	3 Cd(6)	3.051
	1 Cd(25)	3.061
	16, Friauf polyhedron F3	
Cd(25)	6 Cu(1)	2.939
	3 Cu(10)	2.919
	3 Cu(26)	2.941
	3 Cd(19)	3.062
	1 Cd(24)	3.061
	16, Friauf polyhedron F1	
Cu(26)	3 Cu(10)	2.490
	3 Cd(19)	2.924
	3 Cd(25)	2.941
	3 Cu(26)	2.530
	12, icosahedron (26)	
Cu(27)	3 Cu(10)	2.547
	3 Cd(11)	2.817
	3 Cd(13)	2.981
	3 X (14)	2.683
	12, icosahedron (27)	
Cu(28)	3 X (12)	2.707
	3 X (14)	2.713
	3 X (16)	2.708
	3 Cu(21)	2.571
	12, icosahedron (28)	
Cd(29)	12 Cu(8)	2.917
	4 Cd(23)	3.072
	16, Friauf polyhedron F5	

of the paper. The two icosahedra have one vertex in common at the center of the pentagonal prism, and each icosahedron center is at an extended pole of that prism. Each additional vertex that is shared between two icosahedra represents the center of a pentagonal prism (which has two atoms at its extended poles), as can be made out on Fig. 6(*c*). Accordingly, thirty-six more pentagonal prisms are created. In twelve of these prisms, two prism faces are deformed in such a way that two more atoms are added as ligands (to provide ligancy 14).

The aggregate shown in Fig. 6(*c*) accordingly represents fourteen icosahedra, thirty pentagonal prisms, each one with two atoms at the poles (ligancy 12), and twelve pentagonal prisms, each of which has two more atoms penetrating two prism faces (ligancy 14).

The second icosahedral complex is shown in Fig. 7. It consists of a set of six pairs of interpenetrating icosahedra. One such pair is shown in Fig. 7(*a*); the two icosahedra are of the kind marked 15 in Fig. 1. Each pair has its center at the vertex of an octahedron of T_d symmetry; accordingly, each one of two diametrically opposed pairs has its fivefold axis (long axis) at a right angle to that of the other [Fig. 7(*b*)]. Four more icosahedra have to be inserted into this complex. Their centers are at the vertices of a regular tetrahedron, and each of these icosahedra shares six triangles with three 'icosahedron pairs' that surround it, as is shown in Fig. 7(*c*). The four icosahedra are of the kind marked 22 in Fig. 1 and are the dark ones in Fig. 7(*c*). Each vertex that is shared between two icosahedron pairs is, again, the center of a pentagonal prism, which has two atoms at the extended poles and two additional atoms that penetrate two of the prism faces (ligancy 14). Several of the pentagonal prisms can be made out in Fig. 7(*b*), especially at the upper left.

The aggregate shown in Fig. 7(*c*) thus represents sixteen icosahedra and eighteen pentagonal prisms.

The cubic unit contains four aggregates of the kind shown in Fig. 6(*c*) and four of the kind shown in Fig. 7(*c*). The former aggregates are arranged about the points $\frac{3}{4}, \frac{3}{4}, \frac{3}{4}$, *etc.* [point set 4(*d*)] and the latter about the points 0, 0, 0, *etc.* [point set 4(*a*)]. Both types of aggregate are connected with one another by shared vertices in such a way that twelve more pentagonal prisms (plus two atoms at the poles, ligancy 12) are formed between each two complexes. The two types of aggregate [Figs. 6(*c*) and 7(*c*)] thus form the infinite three-dimensional framework shown in Fig. 8. The dark icosahedra shown in Fig. 7(*c*) have been omitted from this large model, since they are difficult to insert.

This framework fits into the cavities formed by the Friauf polyhedra as arranged according to Fig. 5. Both frameworks share vertices with one another in such a way that additional coordination shells, most of them icosahedra, are produced that interpenetrate the Friauf polyhedra as well as the icosahedra described above.

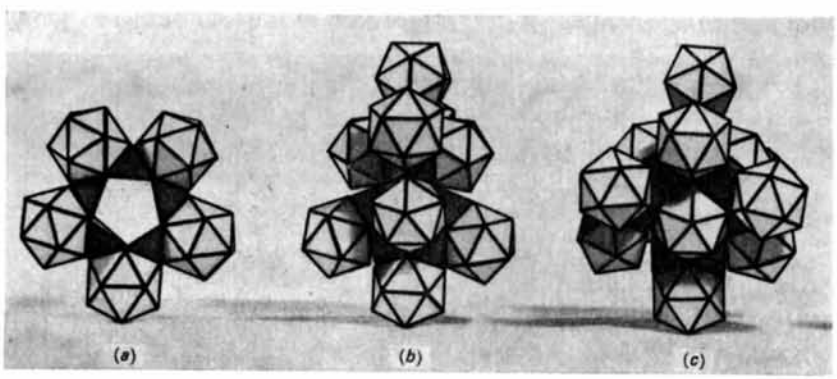

Fig. 6. (*a*) Five icosahedra arranged about an approximate fivefold axis of symmetry. (*b*) Two such fivefold rings interpenetrate at right angles. (*c*) Six interpenetrating fivefold rings form a complex of fourteen icosahedra and forty-two pentagonal prisms.

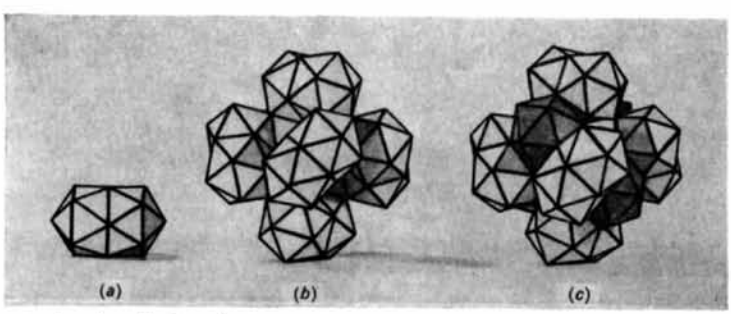

Fig. 7. (*a*) A pair of interpenetrating icosahedra. (*b*) A set of six pairs of interpenetrating icosahedra arranged about the vertices of an octahedron of T_d symmetry. (*c*) Four more icosahedra (dark) arranged with their centers at the vertices of a regular tetrahedron have been added. This aggregate represents sixteen icosahedra and eighteen pentagonal prisms.

Discussion of the coordination polyhedra

The unit cube of structure contains 568 centered icosahedra (ligancy 12); 168 centered pentagonal prisms, each one with two atoms at the extended poles (ligancy 12); 120 centered pentagonal prisms, each one with two atoms at the extended poles and two additional atoms out from the centers of two prism faces (ligancy 14); 144 centered polyhedra of ligancy 15; and 124 Friauf polyhedra (ligancy 16). Each polyhedron of ligancy 15 is a hexagonal antiprism that has one atom out from the center of one hexagon and two atoms out from the other hexagon, which is larger than the first one. This polyhedron was first observed in the μ phase W_6Fe_7 (Arnfelt & Westgren, 1935) and shall be called the μ-phase polyhedron.

The icosahedra and pentagonal prisms

All the 288 pentagonal prisms of the two kinds described above ($L12$ and $L14$) and the 120 icosahedra forming the framework shown in Fig. 8 interpenetrate. Each icosahedron of the kind (28) is penetrated by as many as twelve pentagonal prisms while each of the others is penetrated by either six or four such prisms.

Of the remaining 448 icosahedra 64 are associated solely with the Friauf polyhedra while 384 penetrate both frameworks shown in Figs. 5 and 8; that is, each of these icosahedra has its center at a vertex that is shared between the two frameworks. Similarly, each of the 144 coordination shells of ligancy 15 (μ-phase polyhedra) has its center at such a shared vertex.

Some metrical data on the various kinds of polyhedra are given in Tables 5 to 9.

All but two of the fourteen crystallographically different icosahedra listed in Table 5 have a D/E ratio which is somewhat smaller than that corresponding to a regular icosahedron (0·951), and in each case about half the vertices are occupied by large atoms (cadmium) and the other half by small atoms (copper). A similar distribution of large and small atoms among the icosahedron vertices is observed in the structure of β-Mg_2Al_3 (Samson, 1965), in which a similar variation in the values of E, D, and D/E is also observed.

The pentagonal prisms of the kind $L12$ (Table 6) correspond to a radius ratio of near unity, while those of the kind $L14$ correspond to a radius ratio of about 1·10; the radius ratio is equal to $2D/E-1$.

The Friauf polyhedra

The arrangement of Friauf polyhedra as shown in Figs. 1 and 5 is conveniently discussed by reference to layers in a similar manner to that described in the article by Samson (1967*b*). Comparison of Figs. 1 and 5 of this paper with Fig. 3 in that article shows that the layering of the Friauf polyhedra observed here corresponds to a mixture of the $C14$, $C15$, and $C36$ ($MgZn_2$, $MgCu_2$, $MgNi_2$) types of structure. Other features that these Friauf polyhedra have in common with those observed in the three structure types just mentioned are: (*a*) each vertex of any one truncated tetrahedron represents the center of an icosahedron; (*b*) each of the four hexagons forming a truncated tet-

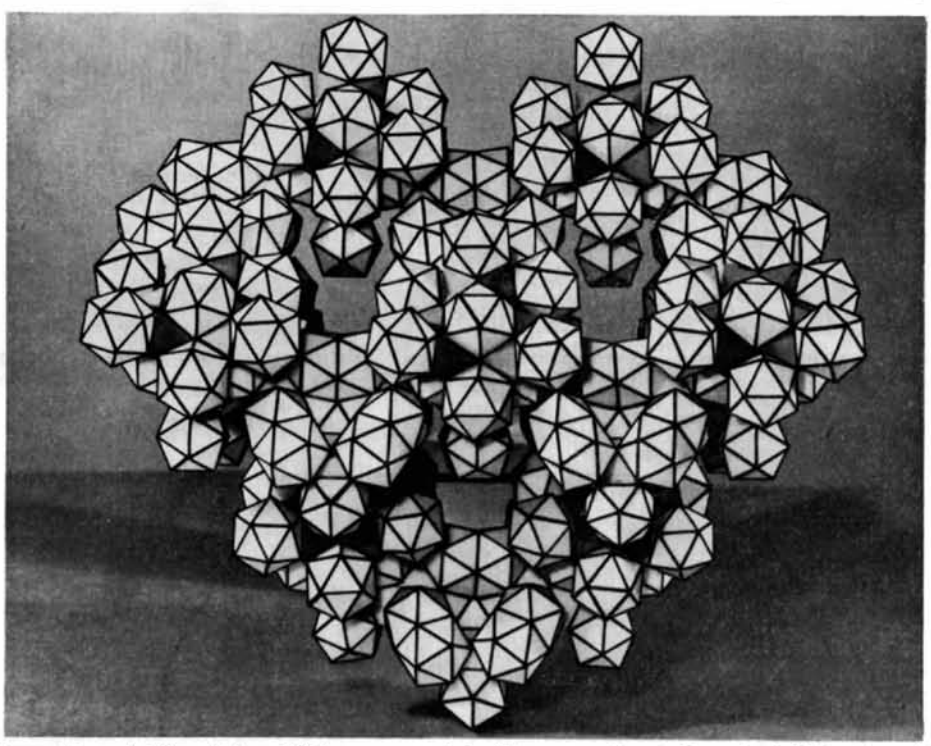

Fig. 8. The complexes shown in Figs. 6(*c*) and 7(*c*) are connected with one another to form the infinite, three-dimensional framework shown here. This framework fits into the cavities formed by the Friauf polyhedra shown in Fig. 5.

rahedron is practically planar; the maximum deviation from any one of the least-squares planes of the eight crystallographically different hexagons involved here is 0·023 Å; (*c*) each hexagon is fairly regular (the shortest side is 2·438 Å, the longest is 2·531 Å); (*d*) the dihedral angle between each two hexagons is nearly tetrahedral (columns 7 and 8, Table 8); (*e*) the interatomic distances between the cadmium atoms of the Friauf framework are fairly equal ($d_{min}=2·933$ Å, $d_{max}=3·076$ Å).

Table 5. *Metrical data on the icosahedra observed in* Cu_4Cd_3

ID = identification number (see Table 4). *N* = number of icosahedra per unit cell, *E* = average length of the 30 edges, *D* = average value of the twelve center-to-vertex distances, Cd, Cu = number of respective atom at the vertices; the fractional numbers result from substitutional disorder.

ID	*N*	*E*	*D*	*D*/*E*	Cd	Cu
1	96	2·903	2·746	0·946	7	5
3	48	2·812	2·665	0·948	5	7
4	48	2·858	2·706	0·947	6	6
5	48	2·852	2·701	0·947	$6\frac{1}{3}$	$5\frac{2}{3}$
7	48	2·861	2·707	0·946	$6\frac{2}{3}$	$5\frac{1}{3}$
8	48	2·861	2·706	0·946	6	6
9	48	2·858	2·707	0·947	6	6
10	48	2·863	2·710	0·947	6	6
15	48	2·883	2·731	0·947	7	5
20	24	2·912	2·756	0·947	7	5
22	16	2·825	2·688	0·952	6	6
26	16	2·876	2·721	0·946	6	6
27	16	2·908	2·757	0·948	$7\frac{1}{2}$	$4\frac{1}{2}$
28	16	2·813	2·675	0·951	5	7
	568					

Table 6. *Metrical data on the two kinds of pentagonal prisms observed in* Cu_4Cd_3

L = ligancy; all other column headings have a similar meaning to those in Table 5. *L*12 arises from two atoms at the extended poles and *L*14 from two additional atoms out from the center of two prism faces.

ID	*N*	*L*	*E*	*D*	*D*/*E*	Cd	Cu
12	48	12	2·940	2·927	0·996	$8\frac{1}{6}$	$3\frac{5}{6}$
14	48	12	2·832	2·828	0·999	$5\frac{2}{3}$	$6\frac{1}{3}$
16	48	12	2·890	2·878	0·996	$6\frac{5}{6}$	$5\frac{1}{6}$
21	24	12	2·701	2·679	0·992	3	9
11	48	14	2·831	2·952	1·043	6	8
17	48	14	2·853	2·995	1·050	8	6
18	24	14	2·857	3·010	1·054	$8\frac{2}{3}$	$5\frac{1}{3}$
	288						

In his study of the geometrical properties of AB_2 structures of the types *C*14, *C*15, and *C*36, Schulze (1958, 1959) discovered the relationship

$$Q=\frac{d_{AB}}{0·5(d_A+d_B)}=1·054,$$

where d_{AB} is the observed distance between a large atom A and the small atom B (here, Cd–Cu or *D* in Table 8), d_A is the observed distance between the large atoms (here Cd–Cd, column 9, Table 8), and d_B between the small atoms (here Cu–Cu or *E* in Table 8). The *Q* values obtained here for the individual Friauf polyhedra are given in column 10 of Table 8; the overall *Q* value is 1·055.

It seems that the cadmium atoms are elongated in the directions of the twelve Cd–Cu bonds and shortened in the direction of the four tetrahedral Cd–Cd bonds. A similar aspherical shape is observed in the elementary (hexagonal) structure of cadmium, in which each cadmium atom forms six long bonds of 3·293 Å and six short bonds of 2·979 Å. A Friauf polyhedron in which the central cadmium atom would employ twelve bonds of the long type with spherical copper atoms of assumed radius 1·278 Å (as in pure copper) and four bonds of the short type with the tetrahedrally arranged cadmium atoms would exhibit the following properties:

$$Q(\text{calc.})=\frac{d_{AB}(\text{calc.})}{0·5[d_A(\text{calc.})+d_B(\text{calc.})]}=\frac{2·925}{0·5(2·979+2·556)}=1·057$$

The observed properties are

$$Q(\text{avg.})=\frac{D(\text{avg.})}{0·5[d_A(\text{avg.})+E(\text{avg.})]}=\frac{2·924}{0·5(3·046+2·496)}=1·055$$

Table 7. *Metrical data on the coordination polyhedra of ligancy* 15 (*μ-phase polyhedra*) *observed in* Cu_4Cd_3

All column headings have a similar meaning to those in Table 5.

ID	*N*	*E*	*D*	*D*/*E*	Cd	Cu
2	96	2·790	2·992	1·072	$6\frac{1}{2}$	$8\frac{1}{2}$
13	48	2·799	2·988	1·067	$6\frac{1}{2}$	$8\frac{1}{2}$

Table 8. *Metrical data and dihedral angles of the truncated tetrahedra observed in* Cu_4Cd_3

The column headings ID, *N*, *E*, *D*, and *D*/*E* have a similar meaning to those in Table 5. There are eighteen edges (*E*) and twelve center-to-vertex distances (*D*). The dihedral angles given in columns 7 and 8 are those between the hexagons; these are nearly planar. d_A = average length of the four Cd–Cd bonds. $Q=D/0·5(d_A+E)$; see text.

ID	Central atom	*N*	*E*	*D*	*D*/*E*	Dihedral angles		d_A	*Q*
*F*1	Cd(25)	16	2·506	2·935	1·171	70·3	70·8	3·062	1·054
*F*2	Cd(19)	24	2·495	2·926	1·173	70·8	70·7	3·028	1·059
*F*3	Cd(24)	16	2·500	2·926	1·171	70·1	71·0	3·054	1·054
*F*4	Cd(6)	48	2·495	2·922	1·171	69·2	69·8	3·012	1·061
*F*5	Cd(29)	4	2·482	2·917	1·175	70°32′*	70°32′*	3·072	1·050
*F*6	Cd(23)	16	2·495	2·916	1·169	70·8	71·0	3·050	1·052
		124							

* Tetrahedral by symmetry requirements.

Table 9. *Metrical data on the Friauf polyhedra*

All column headings have a similar meaning to those in Table 5. There are 48 edges (E) and 16 center-to-vertex distances (D).

ID	E	D	D/E
$F1$	2·749	2·966	1·079
$F2$	2·733	2·951	1·080
$F3$	2·742	2·959	1·079
$F4$	2·729	2·944	1·079
$F5$	2·740	2·956	1·079
$F6$	2·734	2·949	1·079

The close coincidence of the two Q values may be accidental. The average Cd–Cd distance of 3·046 Å observed here is a geometrical requirement for the close packing of Friauf polyhedra in which the average edge of each truncated tetrahedron is 2·496 Å, that is significantly shorter than the Cu–Cu bond of 2·556 Å observed in pure copper.

General discussion of the structure

An interesting feature of this structure is the pronounced tendency toward the creation of fivefold axes, not only those of the icosahedra and pentagonal prisms, but also those of the icosahedral complexes shown in Fig. 6. This striving toward pentagonality is also reflected in the electron density section shown in Fig. 3. The same feature is also observed in the very complex structures of $Mg_{32}(Zn, Al)_{49}$ (Bergman *et al.*, 1957), $NaCd_2$ (Samson, 1962), and β-Mg_2Al_3 (Samson, 1965) and may be due to repulsions between atoms at nonadjacent corners of polygons (Pauling, private communication). With atoms arranged at a distance a at the corners of a square, the next-nearest-neighbor distance is 1·41 a, while in a pentagonal arrangement it is 1·62 a. In a triangular arrangement there are no unbonded neighbors to produce repulsion. This may be a second and perhaps even more important factor than the shortened center-to-vertex distance stabilizing the icosahedral coordination shell with its twenty triangular faces and its six fivefold axes.

The different types of structure that owe their stability to Friauf polyhedra and icosahedra are: (1) $MgCu_2$, $MgZn_2$ (Friauf phases), Friauf (1927*a*, *b*); (2) $MgNi_2$ (Laves phases), Laves & Witte (1935); (3) Mg(Cu, Al), Komura (1962); (4) W_6Fe_7 (μ phases), Arnfelt & Westgren (1935); (5*a*) P (Mo–Ni–Cr) (P phases), Shoemaker, Shoemaker & Wilson (1957); (5*b*) δ (Mo–Ni) (δ phases, closely related to P phases), Shoemaker & Shoemaker (1963); (6*a*) $Mg_3Cr_2Al_{18}$ compounds, Samson (1958, 1961); (6*b*) α-VAl_{10} [closely related to (6*a*)], Brown (1957); (7*a*) α-Mn (χ phases), Bradley & Thewlis (1927); (7*b*) γ-$Mg_{17}Al_{12}$ [closely related to (7*a*)], Laves, Löhberg & Rahlfs (1934); (8*a*) R (Mo–Co–Ni) (R phases), Komura, Sly & Shoemaker (1960); (8*b*) ε-$Mg_{23}Al_{30}$ (closely related to R phases), Samson & Gordon (1967); (9) $Mg_{32}(Zn, Al)_{49}$, Bergman *et al.* (1957); (10*a*) $NaCd_2$, Samson (1962); (10*b*) β-Mg_2Al_3 (closely related to $NaCd_2$), Samson (1965); (11) Cu_4Cd_3 (present work).

The structural relationships between these types of compound have been discussed in detail by Samson (1967*b*).

I thank Mr K. Christiansson and Mrs B. Christiansson for their successful efforts to prepare the single crystals and for other experimental work carried out for this investigation.

References

Arnfelt, H. & Westgren, A. (1935). *Jernkont. Ann.* **119**, 185.
Bergman, G., Waugh, L. T., & Pauling, L. (1957). *Acta Cryst.* **10**, 254.
Bond, W. L. (1951). *Rev. Sci. Instrum.* **22**, 344.
Borg, R. (1961). *A.I.M.E. Trans.* **221**, 527.
Bradley, A. J. & Thewlis, J. (1927). *Proc. Roy. Soc.* A, **115**, 456.
Brown, P. J. (1957). *Acta Cryst.* **10**, 133.
Dauben, C. N. & Templeton, D. H. (1955). *Acta Cryst.* **8**, 841.
Dey, B. N. & Quader, M. A. (1963). *Indian J. Phys.* **37**, 282.
Dey, B. N. & Quader, M. A. (1965). *Acta Cryst.* **18**, 572.
Duchamp, D. J. (1964). *ACA Meeting, Bozeman, Montana*, paper B-14, p. 29.
Friauf, J. B. (1927*a*). *J. Amer. Chem. Soc.* **49**, 3107.
Friauf, J. B. (1927*b*). *Phys. Rev.* **29**, 34.
Hambling, P. G. (1953). *Acta Cryst.* **6**, 98.
International Tables for X-Ray Crystallography (1962). Vol. III. Birmingham: Kynoch Press.
Jenkins, C. H. M. & Hanson, D. J. (1924). *J. Inst. Met.* **31**, 257.
Komura, Y. (1962). *Acta Cryst.* **15**, 770.
Komura, Y., Sly, W. G. & Shoemaker, D. P. (1960). *Acta Cryst.* **13**, 575.
Kripyakevich, P. I., Gladyshevskii, E. I., & Cherkashin, E. E. (1952). *Doklady Akad. Nauk SSSR*, **82**, 253.
Laves, F., Löhberg, K. & Rahlfs, P. (1934). *Nachr. Ges. Wiss. Göttingen, Fachgr. IV*, **1**, 67.
Laves, F. & Moeller, K. (1938). *Z. Metallk.* **30**, 232.
Laves, F. & Witte, H. (1935). *Metallwirt.* **14**, 645.
Owen, E. A. & Pickup, L. (1933). *Proc. Roy. Soc.* A, 139, 526.
Perlitz, H. (1944). *Nature, Lond.* **154**, 607.
Perlitz, H. (1946). *Chalmers Tekniska Högskolas Handlingar*, **50**, 1.
Peterson, S. W. & Levy, H. A. (1957). *Acta Cryst.* **10**, 70.
Samson, S. (1958). *Acta Cryst.* **11**, 851.
Samson, S. (1961). *Acta Cryst.* **14**, 1229.
Samson, S. (1962). *Nature, Lond.* **195**, 259.
Samson, S. (1964). *Acta Cryst.* **17**, 491.
Samson, S. (1965). *Acta Cryst.* **19**, 401.
Samson, S. (1966). *Rev. Sci. Instrum.* **37**, 1255.
Samson, S. (1967*a*). *Rev. Sci. Instrum.* In the press.
Samson, S. (1967*b*). *Structural Chemistry and Molecular Biology*. San Francisco: W. H. Freeman and Company. In the press.
Samson, S. & Gordon, E. K. (1967). Manuscript in preparation.
Shoemaker, C. B. & Shoemaker, D. P. (1963). *Acta Cryst.* **16**, 997.
Shoemaker, D. P., Shoemaker, C. B. & Wilson, F. C. (1957). *Acta Cryst.* **10**, 1.
Schulze, G. E. R. (1958). *Z. Kristallogr.* **111**, 249.
Schulze, G. E. R. (1959). *Freiberger Forschungshefte*, B, **37**, 78.
Webb, N. C. (1964). *Acta Cryst.* **17**, 69.